Volume 66, Issue 1, 2022

Journal of Scientific Research

of

The Banaras Hindu University

Application of High-Resolution X-ray Diffractometry in Measurements of Residual Stress and Strain Rate on Deformed Quartz from Malanjkhand Copper Deposit, India

Dinesh Pandit

Department of Geology, Institute of Science, Banaras Hindu University, Varanasi - 221005, India, Email ID: dpandit@hotmail.com

Abstract: **The Malanjkhand copper deposit is formed due to hydrothermal processes by scavenging metals from the surrounding granitoids. Present study is based on the field observations, quartz recrystallization texture, ore petrography and stress-strain measurements using High-Resolution X-ray Diffractometry (HR-XRD) techniques. Field investigation and quartz recrystallization texture suggest that extensively deformed quartz reef has under gone multiple episodes of tectonic activitiesthat experienced external stress between 12 MPa to 386 MPa in the shallow crustal level. Inhomogeneous strain localization with variable magnitude measured on the quartz samples from the Malanjkhand, up to 2×10^{4}με was recorded along 45º to 75º from normal to the strike of the quartz reef due to external stress. The measured strain-rates in the quartz reef have higher values than the geological strain-rates within the range 1.78×10^{-13} s^{-1} at 250º C to $1.74\times10^{-4}s^{-1}$ at 400ºC. The long-term crustal scale multiple episodes of tectonic events that lead to the development of CIS also show their imprint on the ore bearing quartz reef that results ingrowth of the arcuate shape at the Malanjkhand copper deposit.**

Index Terms: **Deformation; Quartz; Stress; Strain; HR-XRD.**

I. INTRODUCTION

The evolution of orogenic belts due to collisional or extensional plate tectonic depends upon strength and rheology of the continental/oceanic lithosphere (Kirby 1985; Meissner and Wever, 1988; Kusznir et al., 1991; Regenauer-Lieb et al. 2006). Although orogeny involves plate tectonics, either convergent or divergent forces result in a variety of associated geological processes including magmatism, mylonitization, metamorphism, crustal melting and reworking as migmatites (Condie 1997). The association of granites with crustal-scale shear zones is one of the common features observed in the orogenic belts (Brown and Solar 1998). Reconstructing the tectonic history of the granite as well as the evolution of mobile belts needs quantification of geodynamic processes which includes the estimation of pressure, temperature, stress, strain, strain rate and so on.

The High-Resolution X-ray Diffraction (HR-XRD) technique is one of the advanced methodswidely used for identification and characterization of synthetic as well as geological materials. In this study, the HR-XRD technique is used in estimation of geodynamic parameters for reconstruction of the tectonic history of ore bearing quartz reef and rationalize in the context of regional scale tectonics.

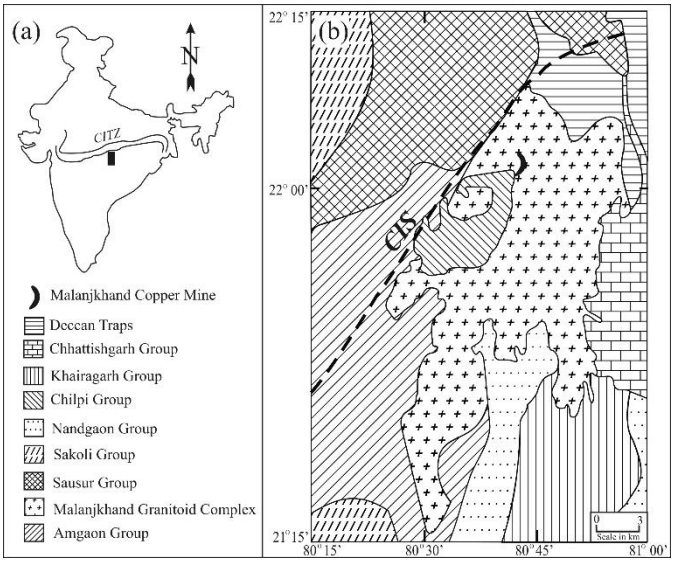

Fig. 1. (a) Map of India showing locations of Malanjkhand granite. (b) General geological map of Malanjkhand granite shows location of quartz reef. CIS is the southern margin in the CITZ (after Acharyya and Roy, 2000).

II. REGIONAL GEOLOGY

The present study is focused on three major lithounits such as Malanjkhand granite (2.48 Ga, Panigrahi et al. 2004, 2009), Central Indian Suture/Shear (CIS) and quartz reef. The study area located in the southern part of the Central Indian Tectonic

Zone (CITZ; Fig. 1a) comprises of two important tectonic units are CIS and Malanjkhand granite (Fig. 1b). The Paleoproterozoic Malanjkhand granite hosts the Cu-Mo-Au bearing arcuate shape quartz reef boarded by CIS in the western-northwestern boundary (Pandit and Panigrahi 2012; Pandit et al. 2014a, b;Pandit 2018). The CIS comprises steeply northward dipping shear zones characterized by multiple bands of mylonites marked as the northwestern boundary of Malanjkhand granite and separates from Sausar mobile belt (Ramachandra and Roy 2001). Two prominent ultra-high temperature metamorphic events (Paleoproterozoic ~2.09 – 2.04 Ga and Mesoproterozoic ~1.52 – 1.45 Ga) are recorded based on the study of monazite geochronology from Sausar mobile belt (Bhowmik et al., 2005). On the other hand, Neoproterozoic age (~0.83 Ga) is recorded from amphibolite facies rocks of Tirodi Biotite Gneiss (Roy et al. 2006).

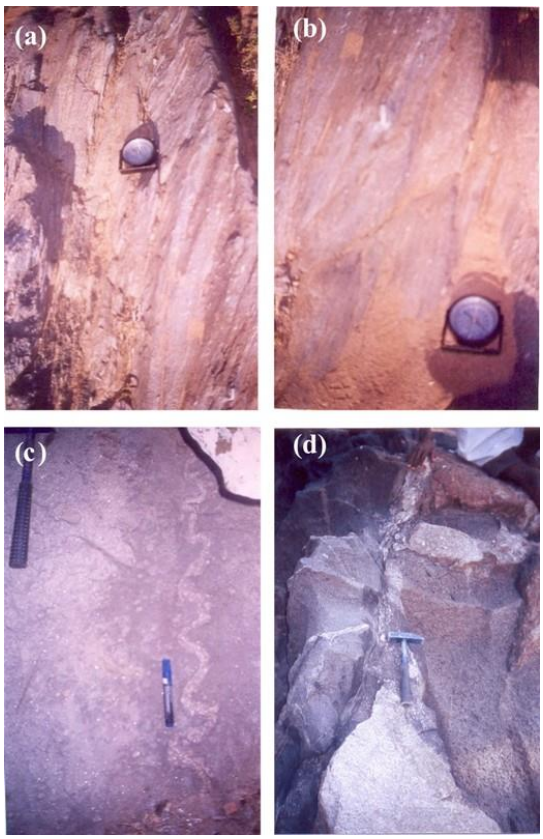

Fig. 2. Field photographs of CIS in north-western boundary of the Malanjkhand granite shows: (a) mylonitic foliations in W-boundary, (b) mylonitic foliations in NW boundary, (c) ptygmatic folds in gneisses, and (d) migmatites.

Prominent features of CIS observed in the mylonitic zones (Fig. 2a and 2b) occurred in the west-northwest margin of the Malanjkhand granite. Mylonitesare N-S trending in the western boundary, NE-SW trending in the northwestern and ENE-WSW trending in the northern boundary of Malanjkhand granite indicates a high strain zone. These are fine grained foliated rocks steeply dipping towards W-NW (Fig. 3a). Metabasic rock has undergone intense shearing with development of quartz bands (Fig. 3b). The basement gneissic rocks are present adjacent to western and northwestern side of the CIS shows characteristics migmatites (Fig. 2d), gneissic bands (Fig. 3c) and ptygmatic folds (Fig. 2c, 3d) were the results of intense deformation and metamorphism. Mylonitization provides constraints to mechanical and thermal models for the metamorphic event associated with peak temperature 630ºC at pressure of 400 MPa under strain-rates in between 10^{-10} to 10^{-13} s^{-1} (Hacker et al. 1990; Etheridge and Wilkie 1981). A minimum differential stress-rate could be in the range 10^{-11} to 10^{-9} MPa/s results dynamic recrystallization to form mylonitic rocks (Prior et al. 1990).

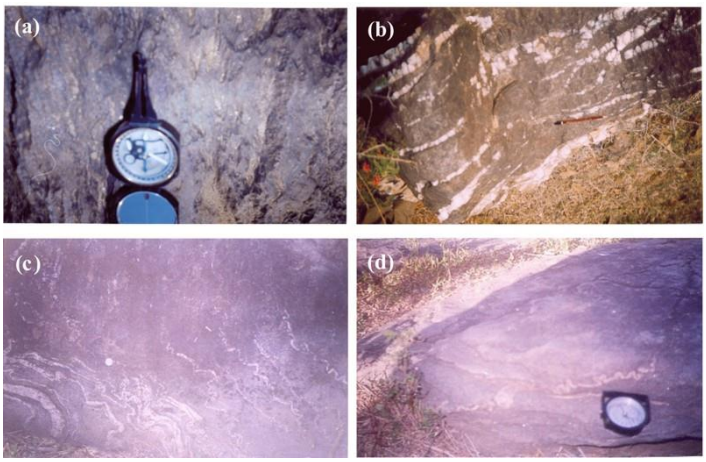

Fig. 3. Field photographs of CIS in northern boundary of the Malanjkhand granite shows: (a) mylonitic foliations, (b) mylonitic quartz veins foliations in northern boundary, (c) migmatitic gneisses, and (d) ptygmatic folds in gneisses.

The N-S oriented Cu-Mo-Au bearing arcuate shape quartz reef is 1.8 km long having an average width of 70 m (Fig. 1b) containing chalcopyrite-pyrite as the main phase of mineralization (Panigrahi et al. 2008). Panigrahi and Mookherjee (1997) reported a dominantly low-temperature (150 to 375ºC) sulfide rich hydrothermal fluid results in the bulk mineralization at 1.1 kbar pressure and extensive silica precipitation in a major fracture zone results in the formation of quartz reef (Panigrahi et al. 2009; Pandit 2014, 2015a, b).

III. Petrography

Quartz microtextures in the photomicrographs show irregular grain shape and variable sizes. Porphyroclasts are referred to as large quartz grains of 2-3 mm in size, which are stretched and elongated. Sample wise photomicrographs of quartz texture is shown in Fig. 4displays deformation and recrystallization within the quartz reef. The recrystallized quartz grains were smaller in size and most of them were <50 μm. The undulatory extinction due to deformation (West 1991) is clearly observed in porphyroclasts but difficult to observe in recrystallized grains under optical microscope. Any special features related to deformation are not observable in recrystallized quartz grains

due to their relative smaller size under optical microscope, however, lattice preferred orientation analysis (LPO) demonstrated variable orientation of quartz grain the Malanjkhand quartz reef (Pandit 2008, 2012).

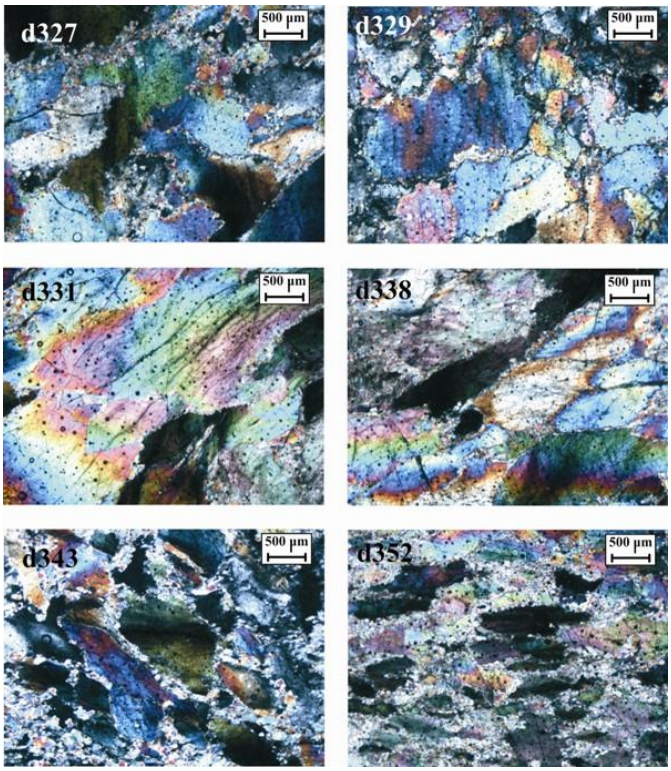

Fig. 4. Photomicrographs (with sample #) showing variation in the pattern of dynamic recrystallization texture in different samples from Malanjkhand reef under cross polarized transmitted light.

Deformational features were also more prominent in ore minerals. Chalcopyrite is the dominant copper bearing ore mineral in association with pyrite, molybdenite, sphalerite, bornite, digenite, chalcocite, covellite, etc. whereas oxide minerals like magnetite and hematite were also observed in Malanjkhand ore bearing quartz reef (Pandit 2015b). Chalcopyrite and pyrite were primary sulfide minerals in association with moderately and intensely oxidized ores in the quartz reef (Sikka et al. 1991). Most of the chalcopyrite and pyrite were fractured and cracks patterns were very prominent (Fig. 5a - d). The observed deformational features in quartz and sulfide minerals need to be quantified in terms of physical constrains like stress and strain. In this situation, X-ray stress measurement method of Sekine and Hayashi (2009) and strain-rate calculation by Hirth et al. (2001) is very useful to investigate geodynamic processes at Malanjkhand.

IV. Theory and Methodology

The external forces either compressive (Fig. 6a) or expansive (Fig. 6b) applied on lattice plane result small change in lattice spacing (Δd). X-ray diffraction technique is one of the established standard procedures to calculate the lattice spacing (d) using the Bragg's law (Fig. 6c). X-ray diffraction spectra were obtained at different tilt angles (ψ) to observe the variation in the d-values. The variation in the d-value is observed in terms of shift in 2θ position on the diffraction spectra (Fig. 6d) and corresponding d-values is calculated using Bragg's law. The $2\theta(rad)$ values were plotted against $sin^2\psi$, the slope (M) of least square fit is used to calculated residual stress (σ_ϕ) using the scheme of Sekine and Hayashi (2009). The lattice spacing (d) is plotted against $sin^2\psi$, the intercept of least square fit is considered as the initial lattice spacing (d_0). The change in lattice spacing (Δd) is obtained by subtracting the measured value of lattice spacing (d) from calculated unstressed lattice spacing (d_0). The Δd is –ve for compressive and +ve for expansive external force (Fig. 9a, b). The ratio of Δd to d_0 is the calculated value of strain (e_i) on surface of the sample. Finally, strain rate is calculated using the formulation of Hirth et al. (2001).

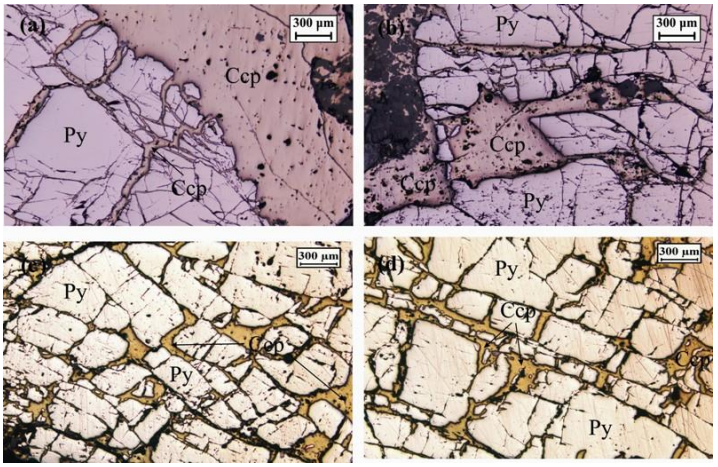

Fig. 5. Photomicrographs from Malanjkhand reef shows deformation features in ore samples under polarized reflected light (Note: Ccp – chalcopyrite, Py – pyrite).

Total 18 oriented quartz samples were collected from the mine pit and selected for phase and residual stress analysis using HR-XRD. X-ray residual stress measurements were conducted using a PAnalyticalX'Pert PRO HR-XRD with a position sensitive detector (PW3011/20 Miniprop large window), goniometer (PW3050/60), and X-ray tube (PW3373/00 Fe LFF DK 147167), using $FeK_{\alpha 1,2\beta}$ radiation in a reflected mode at Central Research Facilities, Indian Institute of Technology Kharagpur. The XRD is calibrated with synthetic α-quartz at 40 kV voltages and 20 mA current. A single sample holder stage (PW3071) is used which is capable of 360° angular movement in X-Y plane (azimuthalangleϕ) and up to 90° angle in YZ plane expressed in terms of tilt angle (ψ) as shown in the Fig. 7(a). The X'Pert Data Collector version 2.0e software with instrument control XPERT PRO version 1.9a program was used for data collection with minimum step size 0.001 in both 2θ and ψ direction. The wavelength $FeK_{\alpha 1}$ = 1.93609 Å and $FeK_{\alpha 2}$ = 1.94003 Å with a ratio of $K_{\alpha 1}/K_{\alpha 2}$ = 0.5 radiation was applied. The radius of the incident beam path as well as diffracted beam path is 240 mm

with Point detector. The analysis was performed in two stages comprising of phase analysis and residual stress analysis.

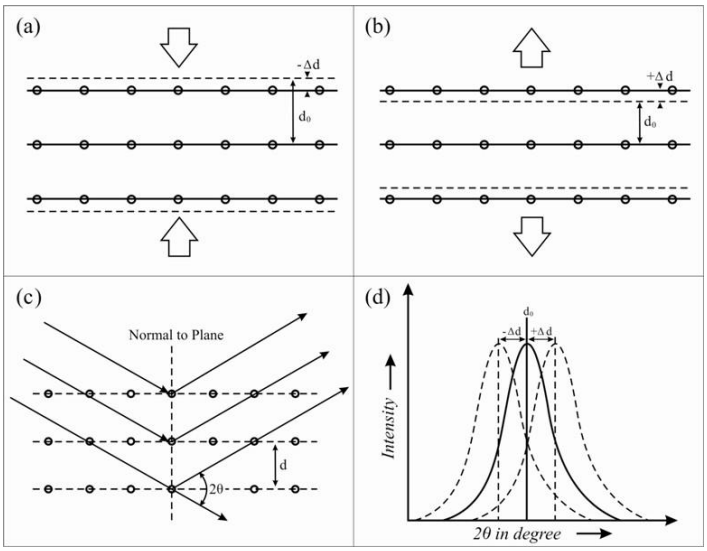

Fig.6. Schematic diagram shows the theory of residual stress measurements: (a) compressive stress on lattice plane, (b) expansive stress on lattice plane, (c) diffraction technique, and (d) -ve or +ve change in the peak position due to applied stress.

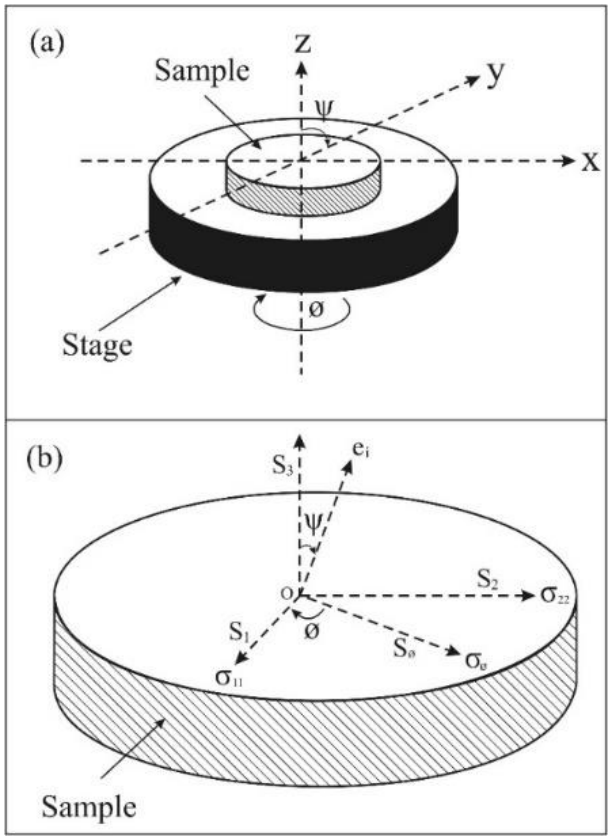

Fig. 7. Schematic diagrams represent residual stress measurements on sample at specific title angles (ψ) and azimuthal angle (ϕ)with respect to stage: (a) orientation of the sample and sample-stage holder represented in coordinate geometry, and (b) orientation of stress and strain components on the sample surface.

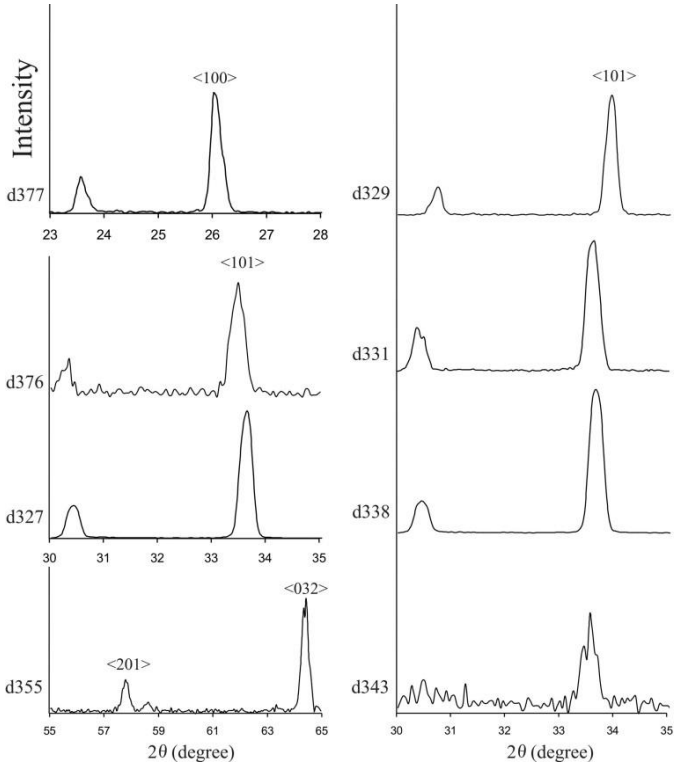

Fig. 8. X-ray diffraction patterns representing <100>, <101>, <201>, and <032> peaks associated with FeKα incident X-ray radiations corresponding to quartz samples. Sample number shows in the left side of the corresponding X-ray patterns.

A. Phase Analysis

The diffracted beam was collected over the range 20° to 70° in 2θ scan for identification of the major peaks in the X-ray diffraction spectra. The resulting spectra were analyzed using PANalyticalX'Pert Data Viewer version 1.0c software working on Rietveld method was used for the identification of the lattice plane. The most intense peak was variable in $2\theta^{o}$ position for different samples observed due to its crystal orientations. In sample no d377, the most intense peak is recorded at 26.025° and sample no d355 having 64.425° corresponds to lattice plane <100> and <032> respectively (Fig. 8) while remaining samples having most intense peak in the range of 33.325° to 33.975° in 2θ scale corresponds to <101> crystallographic planes of α-quartz.

B. Residual Stress Analysis

The intensity of the most intense peak is very good and therefore selected for stress analysis within ±0.5° in 2θ scale in the X-ray diffraction spectra. The diffraction patterns were collected at title angles (ψ) which refers to the angle between the normal directions of the lattice plane exposed to the X-ray beam and the sample surface. The ψ angles are in the range of -90° to +90° in 18 equal intervals of 5.9° in positive as well as negative side from the normal position (ψ = 0°), where the take-off angle is 6°(Pandit 2010). Total 36 spectra were collected at different

tilt angles and analyzed using PANalyticalX'Pert Stress version 1.0a software. The slope M is obtained from a least squares linear fit to peak location and $sin^2\psi$, which is converted into stress magnitude in the tilting direction based on the formulation of Sekine and Hayashi (2009). The stress magnitude in directions corresponding to azimuthal angle (ϕ) at 0° was determined as S_ϕ (Fig. 7b).

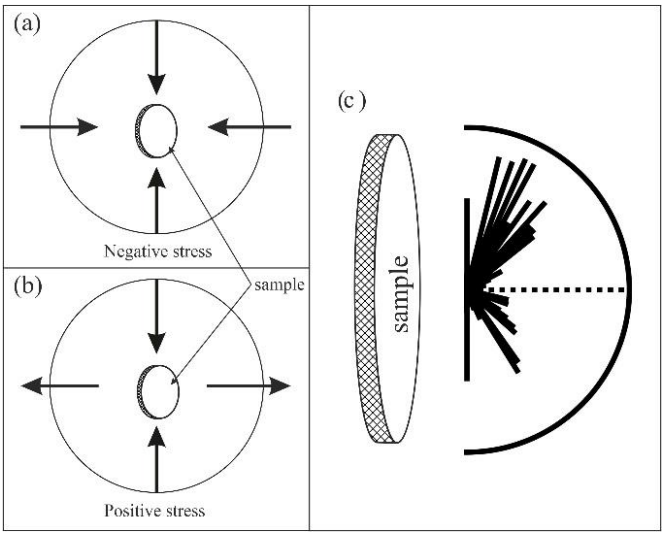

Fig. 9. Schematic diagrams show directions of (a) negative stress and (b) positive stress with respect to fixed normal stress component; and (c) orientation of the magnitude of strain component measured on the sample surface plotted on the polar diagram from -90° to 90° counter clock wise.

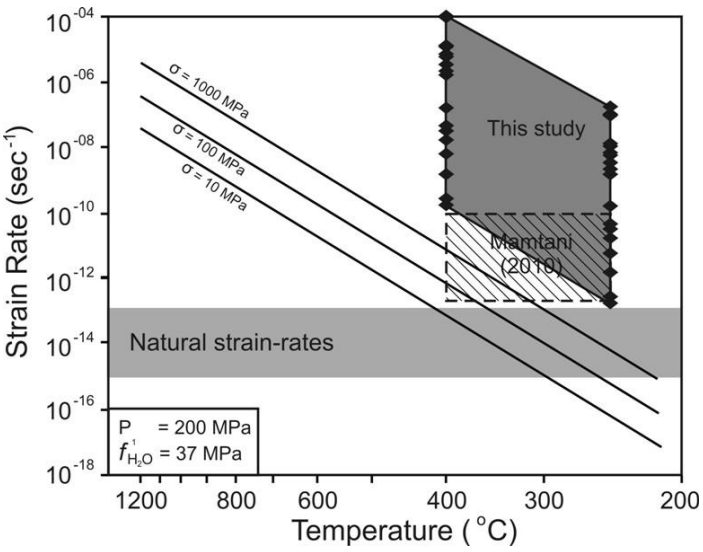

Fig. 10. Estimation of deformation conditions and temperature obtained from bulging recrystallization texture (Stipp et al., 2002) in quartz reef. Theoretical estimates of strain-rates represented by solid lines (Hirth et al., 2001). Calculated strain-rates (solid diamonds) using the formulation of Hirth et al. (2001) represented by filled box area compared with the results of fractal analysis with shaded box area (Mamtani, 2010) against the temperature variations.

V. Results

The Malanjkhand quartz reef is dominated by bulging recrystallization texture of quartz grains indicates that the deformation possibly took place in a temperature range of 250 to 400°C. The main phase of mineralization associated with chalcopyrite-pyrite assemblages hosted in quartz also shows plastically deformed and intensively fractured.

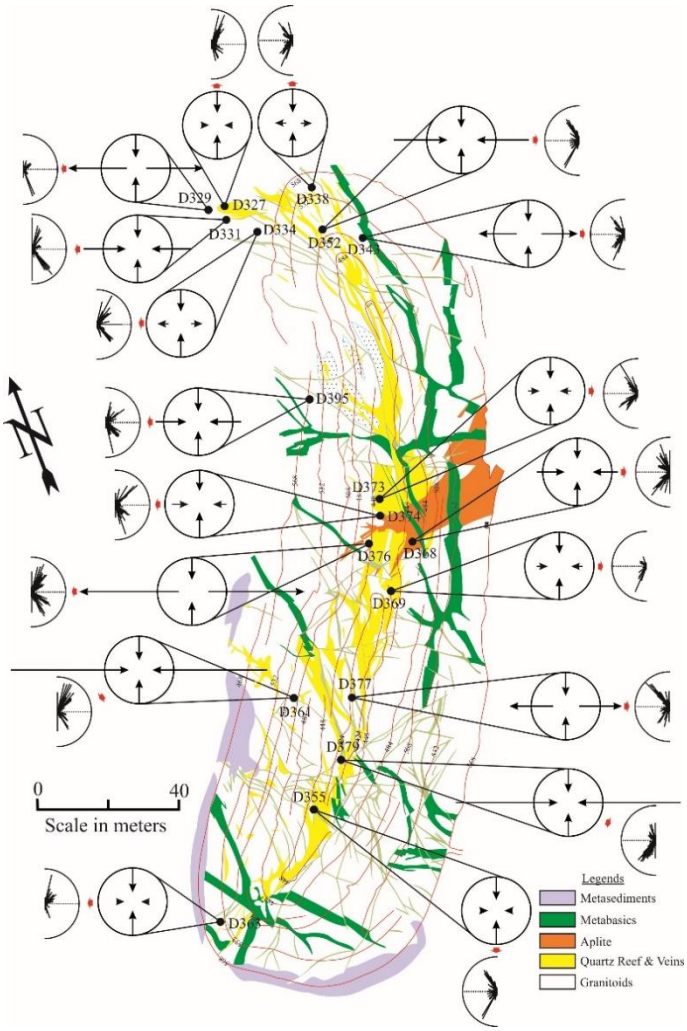

Fig. 12. Stress and corresponding strain patterns obtained in the present study shown on the Malanjkhand quartz reef (Courtesy: Malanjkhand Copper Project, Hindustan Copper Limited, India).

X-ray diffraction patterns of 18 quartz samples were analyzed for identification of crystal lattice plane that corresponds to α-quartz. Response of <101> lattice plane was very well observed while two sample shows their response to <100> and <032> plane for most intense peak. This indicates most of the samples having more or less similar crystallographic orientation except two samples could be considered as the experimental error or orientation of the sample with respect to the mine wall. The unstressed lattice spacing (d_0) for <101> plane is varying in the range of 3.316 to 3.374 Å (Table I).

Table I. Measured crystal lattice parameters <h k l>, unstressed lattice spacing d0(Å), slope (M), stress component (MPa) and strain-rates (s^{-1}) at 250°C and 400°C using the scheme of Hirth et al. (2001) of naturally deformed quartz samples from Malanjkhand.

Sample No.	h k l	d_0 (Å)	Slope (M)	Stress (σ_ϕ) (MPa)	Strain Rate (s^{-1}) 250 °C	400 °C
d327	1 0 1	3.34135	0.00017	-12.31	1.78×10^{-13}	1.79×10^{-10}
d329	1 0 1	3.31590	-0.00272	195.33	1.13×10^{-8}	1.14×10^{-5}
d331	1 0 1	3.35141	0.00225	-163.47	5.53×10^{-9}	5.58×10^{-6}
d334	1 0 1	3.35213	-0.00053	38.52	1.70×10^{-11}	1.72×10^{-8}
d338	1 0 1	3.33775	-0.00029	20.98	1.50×10^{-12}	1.51×10^{-9}
d343	1 0 1	3.35060	-0.00199	144.54	3.38×10^{-9}	3.41×10^{-6}
d352	1 0 1	3.34849	0.00279	-202.51	1.30×10^{-8}	1.31×10^{-5}
d355	0 3 2	1.81842	-0.00129	44.96	3.16×10^{-11}	3.19×10^{-8}
d361	1 0 1	3.35021	0.00532	-386.37	1.73×10^{-7}	1.74×10^{-4}
d363	1 0 1	3.34376	0.00019	-13.77	2.78×10^{-13}	2.81×10^{-10}
d368	1 0 1	3.34900	0.00164	-119.06	1.56×10^{-9}	1.57×10^{-6}
d369	1 0 1	3.34504	0.00068	-49.30	4.58×10^{-11}	4.61×10^{-8}
d373	1 0 1	3.34697	0.00041	-29.75	6.06×10^{-12}	6.11×10^{-9}
d374	1 0 1	3.35015	0.00093	-67.54	1.61×10^{-10}	1.62×10^{-7}
d376	1 0 1	3.34306	-0.00455	329.68	9.15×10^{-8}	9.22×10^{-5}
d377	1 0 0	4.28491	-0.00182	172.03	6.78×10^{-9}	6.84×10^{-6}
d379	1 0 1	3.35500	0.00460	-334.60	9.71×10^{-8}	9.79×10^{-5}
d395	1 0 1	3.37385	0.00176	-128.81	2.13×10^{-9}	2.15×10^{-6}

Estimated residual stress is classified into two different categories such as negative and positive stress, which is related to the compressive (Fig. 9a) and expansive (Fig. 9b) tectonic forces in the presence of uniform lithostatic pressure. The compressive stress is estimated in the range of -12 to -386 MPa while expansive stress is in between 21 to 330 MPa. Overall, the magnitude of the minimum stress is about 12 MPa while that of maximum stress is 386 MPa (Table I).

According to Hook's law, the applied stress is directly related to the strain. The multiple tectonic events associated with compressive as well as expansive forces applied on the quartz reef develop positive as well as negative strain respectively, expressed in terms of microstrain ($\mu\varepsilon$,10^{-6}). The compressive force decreases the lattice spacing which is related to positive strain while the opposite situation appears for negative strain. The microstrain ($\mu\varepsilon$) is measured along the tilt angle (ψ) from -90° to +90°in 18 equal intervals of 5.9° on YZ plane (Fig. 7a). The calculated microstrain ($\varepsilon_i\times10^6$) is perpendicular to the measured stress component (S_ϕ) as shown in Fig. 7b. The magnitude of microstrain is presented in the form of polar diagram directed away from the surface of the sample (Fig. 9c). There are two to three orders of variation in the magnitude of calculated microstrain (Table II), which indicates the nature of deformation was highly inhomogeneous.

Mamtani (2010) suggested the lower limit of strain-rate is about 10 to 12.7 s^{-1} at 250°C for Malanjkhand quartz reef using area-perimeter fractal dimension and suggested higher strain-rate at higher temperatures. The problem is more complicated due to presence of aqueous bi-phase inclusion in the Malanjkhand quartz reef, provide adequate water during deformation (Panigrahi and Mookherjee 1997). Presence of aqueous bi-phase inclusions indicates deformation took place under wet conditions. Hence, the formulation of Hirth et al. (2001) is very useful in these conditions for estimation of strain-rates. Calculated strain-rates were in the range of 10^{-13} to 10^{-7} s^{-1} at 250° C and 10^{-10} to 10^{-4} s^{-1} at 400°C (Table I). The temperature versus strain rate diagrams suggested that the Malanjkhand quartz reef was deformed at confining lithostatic pressure of 200 MPa (Fig. 10). This indicates strain-rates were directly related to temperature which means high strain-rates at higher temperature. There is a six order of variation in the value of strain-rates in the Malanjkhand quartz reef and maximum value is about 10^{-4} s^{-1} at 400°C (Table I) possibly due to multiple tectonic forces appears at inconsistent deformation events.

VI. Discussions

There are different opinions related to the evolutionary history of the CITZ and the style of mineralization at Malanjkhand. Broadly, it can be divided into two categories: (i) fracturecontrolled quartz reef hosted mineralization (Rai and Venkatesh 1990, 1993; Panigrahiand Mookherjee 1997; Vishwakarma 2001; Panigrahi et al. 2008; Pandit et al. 2019) and (ii) porphyry style mineralization (Sikka 1989; Ramnathan et al. 1990; Sarkar et al. 1996; Sikka and Nehru 1997, 2002;

Bhargava and Pal 1999, 2000; Stein et al. 2004, 2006). However, the general opinion is attributed to post depositional brittle-ductile deformation (Sarkar et al. 1996) which resulted in the formation of present shape of the Malanjkhand quartz reef. Panigrahi et al. (2008) suggested that the Malanjkhand deposit represents a fractured filled granitoid-associated ancient/fossil geothermal system based on the physicochemical characteristics of the mineralized fluid and associated mineral chemistry.

The fracture filled quartz reef model, which has undergone extensive deformation during multiple tectonic events, is supported from the field observation, petrography of quartz reef, estimated stress, strain and strain-rates parameters, etc. The calculated stress component (S_ϕ) with respect to lithostatic pressure of 200 MPa and the polar diagrams representing the magnitude of strain along with their stress component is shown in the Fig. 12 which represents a non-uniform pattern within the mine pit. One of the major factors is that the high magnitude of strain inclined around 45º to 75º in both –ve as well as +ve directions from the horizontal (ψ = 0). The magnitude of the stress is more intense towards southern part of the quartz reef. At the edge of the reef, the stress component is very weak compared to other parts of the reef. The nature of the stress component is not regular whether compressive or expansive but frequently observed throughout the reef (Fig. 12). In general, ductile deformation operated at high pressure-temperature with low strain rate (Rutter and Maddock 1992), however, brittle deformation occurs at low pressure-temperature with high strain-rate (den Brok 1998). The observed limiting conditions for deformation at Malanjkhand indicates that the quartz reef has under gone long term multiple tectonic events in upper crustal level thatresulted the present arcuate shape.

Conclusion

The Malanjkhand ore bearing quartz reef is dominated by bulging recrystallization texture which took place at moderate temperature in the rage of 250º to 400ºC. Major sulfide phase constitutes of chalcopyrite and pyrite undergone plastic deformation. The ore bearing reef is made of α-quartz which hosted in the granitic country rock known as Malanjkhand granite. The arcuate shape reef has under gone multiple phases of tectonic events with at least an external stress of 12 MPa but not exceeding 386 MPa that leads to the deformation. The applied stress leads to the development of localized strain patterns around 45º to 75º from normal to strike direction of the quartz reef. Magnitude of the maximum strain varies up to 2×10^4microstrain ($\mu\varepsilon$) but inhomogeneous in nature. The observed negative as well as positive strain on the quartz reef resulted due to compressive as well as expansive forces during multiple tectonic events. Deformation took place with a higher strain-rates compared to the natural strain-rates and it increases with increasing temperature. The maximum strain-rates observed on the reef are about 1.74×10^{-4} s^{-1} at 400ºC while the minimum value is equivalent to upper limit of the geological strain-rates i.e. 1.78×10-13 s^{-1} at 250ºC. All the above parameters define the limiting conditions at which geodynamics processes play their role in the development of the arcuate shape quartz reef within a time period of 1.2 billion years of tectonic history starting from Paleoproterozoic to Neoproterozoic (ca. 2.10 to 0.80 Ga) in Malanjkhand granite. The long-term dynamic interaction between the intervening quartz with the granitic country rock has resulted into the brittle-ductile deformation and strain localization in the ore bearing reef.

Acknowledgment

Author acknowledges the Council of Scientific and Industrial Research, Government of India for financial support in terms of research fellowship. The author also thanks Prof. M. K. Panigrahi, Mr. B. K. Das and staff members of Central Research Facilities, Indian Institute of Technology Kharagpur for their support during the experiment with HR-XRD. Thanks are also to the reviewer for his constructive suggestions.

References

Acharyya, S.K., &Roy, A. (2000). Tectonothermal history of the Central Indian Tectonic zone and reactivation of major fault/shear zones. Journal of the Geological Society of India, 55, 239-256.

Bhargava, M., &Pal, A.B. (1999). Anatomy of a porphyry copper deposit-Malanjkhand, Madhya Pradesh. Journal of Geological Society of India, 53, 675-691.

Bhargava, M., &Pal, A.B. (2000). Cu-Mo-Au metallogeny associated with Proterozoic tectono-magmatism inMalanjkhand porphyry copper district, Madhya Pradesh. Journal of Geological Society of India, 56, 395-413.

Bhowmik, S.K., Sarbadhikari, A.B., Spiering, B., &Raith, M.M. (2005). Mesoproterozoic reworking of Paleoproterozoic ultrahigh temperature granulites in the Central Indian Tectonic Zone and its implications. Journal of Petrology, 46, 1085-1119.

Brown, M., &Solar, G.S. (1998). Shear zone systems and melts: Feedback relations and self-organization in orogenic belts. Journal of Structural Geology, 20, 211-227.

Condie, K.C. (1997). Plate Tectonics and Crustal Evolution, (Fourth Edition). Oxford, PA: Butterworth-Heinemann Publications.

Den Brok, S.W.J. (1998). Effect of microcracking on pressure-solution strain rate: the Gratz grain-boundary model. Geology, 26, 915-918.

Etheridge, M.A., &Wilkie, J.C. (1981). An assessment of dynamically recrystallized grain size as a palaeopiezometer in quartz-bearing mylonite zones. Tectonophysics, 78, 475-508.

Table II: Estimated values of strain at different title angles (ψ) from -90° to +90° using the formulations of Sekine and Hayashi (2009)expressed in microstrain ($e_i \times 10^6$).

ψ°	d327	d329	d331	d334	d338	d343	d352	d355	d361	d363	d368	d369	d373	d374	d376	d377	d379	d395
-90.0	-180	2663	-230	-104	-2918	2098	-1374	764	-8996	-1791	-2899	1641	-1216	-2848	6054	4595	-8185	-2152
-76.4	5875	2578	2873	-1041	8530	-1448	-3643	-1248	-1418	-2838	-6560	1716	-3269	-4486	-3024	5356	-7785	-10904
-70.5	997	20525	-2032	2273	-3050	3602	-3626	2898	-2107	4393	-10128	-4720	-6215	-7170	3383	2163	-7624	-4431
-65.9	5354	19735	134	-1665	-2295	6715	-5877	2992	-3200	-452	5231	-2831	-786	-3385	7694	2588	1514	-4393
-61.9	5090	3788	-859	-644	-3038	8518	-8001	1496	-2949	-449	7450	-1040	-550	2334	9476	2306	2390	-3361
-58.2	2777	-124	-8495	-179	-2490	8318	-8658	2524	-9635	-837	6650	-448	-11918	-4233	8758	5972	2349	-2718
-54.7	865	-2024	-9020	698	7901	6050	-7705	2882	-8779	-416	51	-720	-2062	469	-2148	6238	-4873	-4716
-51.4	-802	-5042	-11156	3810	10486	7118	824	4729	-2460	-751	511	1381	7440	2689	5986	10082	-4355	-6236
-48.2	-2499	-3625	-9136	3786	7517	7840	2210	1914	33	48	7083	-1519	5184	2337	-3335	10292	-3896	-6547
-45.0	-1769	374	-8883	3550	330	3784	-146	781	469	-796	1105	-3199	-5241	-2630	769	11902	-3809	6518
-41.8	3708	4355	1766	3836	192	5384	-2897	1809	-6450	467	-3547	-3154	-4081	45	4517	5741	-2486	6242
-38.6	5025	2675	2691	-1542	-5318	6485	-4059	1276	5970	-1782	-3858	-3877	-4007	3728	6772	233	-2057	3014
-35.3	1299	2642	2432	-1718	425	5047	-708	-71	4841	-550	-1863	1501	-2931	4089	8038	-2560	-4083	4775
-31.8	407	2934	838	-203	5408	430	-1344	2194	3853	-667	-4467	2915	-1643	3033	7206	-948	-3821	6204
-28.1	434	501	746	1569	4464	501	-609	1919	663	-1005	-4676	3563	466	1119	3670	-2712	-1341	2754
-24.1	4423	-1053	415	483	303	1833	-645	181	-2433	-673	-4452	-511	3322	-510	5863	-723	2724	436
-19.5	3023	2370	-1346	298	1459	1916	-487	434	-4307	748	18	-66	2256	-1021	-1783	294	158	-1420
-13.6	2780	1933	-1519	-719	147	1379	3163	423	-4224	-66	-1033	1013	1356	-1907	1313	-1442	-966	-2024
0.0	1784	2681	-337	-4344	1534	537	-3396	110	-454	-413	1490	-628	314	-1206	-640	105	-1231	836
13.6	1903	1439	-3336	-2243	4386	1080	-3563	1617	-1913	-2563	-1377	-1734	651	-1275	329	3018	-2867	-2816
19.5	-886	4457	-3115	498	473	1606	451	-1578	1910	-906	33	-1961	1613	224	-1143	2502	-2385	-3904
24.1	-2062	4005	-3005	128	3137	-2465	765	-2216	-2522	-2572	-917	-726	-4649	394	-2519	2985	-92	-1073
28.1	-2451	5775	-2993	-1232	1046	-4193	-3646	-2222	-3904	-3209	1290	-12	-2525	-1170	-4340	3613	2045	56
31.8	-1565	6985	-1408	659	-4464	-4011	-1541	-2502	-2080	-1247	4136	-828	-7150	-33	-5115	1613	3237	-4227
35.3	-1095	-2572	662	1650	-4590	-2955	72	1490	892	2701	3595	-1175	-8172	-1875	4595	-238	2346	-7881
38.6	-2523	-3764	1086	3237	-261	-2319	1953	-1248	-8408	4268	3040	-4714	2148	-3534	2860	-2331	-4495	-5575
41.8	-2969	-6942	1474	2849	-5986	504	3679	-687	-8907	3616	3491	-3	4264	-6865	4627	-1454	-3848	-2676
45.0	-3750	-4907	1689	2777	-8488	30	-3835	-341	-8892	3670	-8388	272	5653	-6173	3368	3594	-8063	-910
48.2	-4142	-1629	2360	522	-6606	585	-1855	1144	-11602	1570	-7232	1088	5220	-2328	7948	-196	-12164	-2940
51.4	-6901	392	5401	-3747	-7883	-3528	-1768	2238	-3212	1657	-10322	3611	6182	-248	7595	-3207	-9839	-4840
54.7	-5210	1915	5022	-2279	-7796	-5217	-1595	-2596	-10707	-18	-6530	6155	7057	-525	6383	-7013	-11860	-2700
58.2	-6117	1831	21	352	-4928	-8196	-9930	-456	-7782	3894	-2440	6921	2605	5236	7466	-6437	-11362	-368
61.9	-8128	2473	1564	5662	-2328	3247	-10709	-594	-14041	3338	-7184	703	457	1495	7616	567	-9079	1971
65.9	-11097	4949	-7182	2530	13057	4131	-2765	-1589	-14133	1447	4604	-12843	-496	1042	10538	1333	-9255	3441
70.5	5411	6737	-7642	650	9102	4011	-2494	-242	-13408	-4573	2359	-7067	-2970	-839	9336	4857	-7914	5747
76.4	10367	1092	-8301	-4021	1249	1501	-3004	654	-13471	-8556	-7307	2051	1867	-3833	8941	7116	-6894	-7268
90.0	-1745	6140	-10954	695	1094	3125	-541	577	-1683	-425	-7489	-1596	-756	725	7062	5342	-3705	-1227

Hacker, B.R., Yin. A., &Christie, J.M. (1990). Differential stress, strain rate, and temperature of mylonitization in the Ruby Mountains, Nevada: implications for the rate and duration of uplift. Journal of Geophysical Research, 95, 8569-8580.

Hirth, G., Teyssier, C., &Dunlap, W.J. (2001). An evaluation of quartzite flow laws based on comparisons between experimentally and naturally deformed rocks. International Journal of Earth Science,90, 77-87.

Kirby, S.H. (1985). Rock mechanics observations pertinent to the rheology of the continental lithosphere and the localization of strain along shear zones. Tectonophysics, 119, 1-21.

Kusznir, N.J., Vita-Finzi, C., Whitmarsh, R.B., England, P., Bott, M.H.P., Govers, R., Cartwright, J., &Murrell, S. (1991). The distribution of stress with depth in the lithosphere: thermo-rheological and geodynamic constraints [and discussion]. Philosophical Transactions: Physical Science and Engineering, 337, 1645, 95-110.

Mamtani, M.A. (2010). Strain-rate estimation using fractal analysis of quartz grains in naturally deformed rocks. Journal of Geological Society of India,75, 202-209.

Meissner, R., &Wever, T. (1988). Lithospheric rheology: continental versus oceanic unit. Journal of Petrology Special Volume, 1, 53-61.

Pandit, D. (2008). A comparative study of the Paleoproterozoic Malanjkhand and Dongargarh Granitoids, Central India: Implications to Crustal Evolution and Metallogeny. Ph. D. thesis. IIT Kharagpur Online: http://www.idr.iitkgp.ac.in/xmlui/handle/123456789/408;http://eprints.csirexplorations.com/217/.

Pandit, D. (2010). Residual stress and strain rate measurements on deformed quartz using High-Resolution X-ray Diffractometry. 7th Annual Meeting, Asia Oceania Geosciences Society Hyderabad India, SE09-A008, p294.

Pandit, D. (2012). Lattice preferred orientation analysis of deformed quartz using X-ray Texture Goniometry: an advanced application of High Resolution X-ray Diffractometer. Journal of the Geological Society of India, 79, 169-174.

Pandit, D. (2014). Chloritization in Paleoproterozoic granite ore system at Malanjkhand, Central India: mineralogical studies and mineral fluid equilibria modeling. Current Science, 106, 565-581.

Pandit, D. (2015a). Thermodynamic model for hydrothermal sulfide deposition in the Paleoproterozoic granite ore system at Malanjkhand, India. Indian Journal of Geo-Marine Sciences, 44 (11), 1697-1711.

Pandit, D. (2015b). Geochemistry of feldspar intergrowth microtextures from Paleoproterozoic granitoids in Central India: implications to exsolution processes in granitic system. Journal of the Geological Society of India, 85, 163-182.

Pandit, D. (2018). Crystallization evolution of accessory minerals in Paleoproterozoic granites of Bastar Craton, India. Current Science, 114 (11), 2329-2342.

Pandit, D., &Panigrahi, M.K. (2012). Comparative petrogenesis and tectonics of Paleoproterozoic Malanjkhand and Dongargarh granitoids, Central India. Journal of Asian Earth Sciences, 50, 14-26.

Pandit, D., Bhattacharya, S., &Panigrahi, M.K. (2019). Dissecting through the metallogenic potentials of older granitoids - case studies from Bastar and Eastern Dharwar cratons India Archean Granitoids of India: Windows into Early Earth Tectonics. Archean Granitoids of India: Windows into Early Earth Tectonics, Geological Society of London Special Publication, 489, 157-188. https://doi.org/10.1144/SP489-2019-342.

Pandit, D., Panigrahi, M.K., & Moriyama, T. (2014a) Constrains from magmatic and hydrothermal epidotes on crystallization of granitic magma and sulfide mineralization in Paleoproterozoic Malanjkhand granitoid, Central India. Chemie der Erde/Geochemistry, 74, 715-733.

Pandit, D., Panigrahi, M.K., Moriyama, T., &Ishihara, S. (2014b). A comparative geochemical, magnetic susceptibility and fluid inclusion studies on the Paleoproterozoic Malanjkhand and Dongargarh granitoids, Central India and implications to metallogeny. Mineralogy and Petrology, 108, 663-680.

Panigrahi, M.K., &Mookherjee, A. (1997). The Malanjkhand copper (+molybdenum) deposit, India: Mineralization from a low-temperature ore-fluid of granitoid affiliation. Mineralium Deposita,32, 133-148.

Panigrahi, M.K., Bream, B.R., Misra, M.C., &Naik, R.K. (2004). Age of granitic activity associated with copper-molybdenum mineralization at Malanjkhand, Central India. Mineralum Deposita, 39, 670-677.

Panigrahi, M.K., Pandit, D., &Naik, R.K. (2009). Genesis of the granitoid affiliated Paleoproterozoic copper-molybdenum deposit at Malanjkhand: A review of status. In S. Kumar (Ed.), Magmatism, Tectonism and Mineralization (pp. 265-292). Delhi, PA: Macmillan Publisher India Ltd.

Prior, D.J., Knipe, R.J., Handy, &M.R. (1990). Estimates of the rates of microstructural changes in mylonites. Geological Society London Special Publications, 54, 309-319.

Rai, K.L., &Venkatesh, A.S. (1990). Malanjkhand copper deposit: a petrological and geochemical appraisal. Geological Survey of India Special Publications, 28, 563–584.

Rai, K.L., &Venkatesh, A.S. (1993). Geological setting and nature of copper–molybdenum mineralization in the intra-

continental acid magmatic regime of Malanjkhand, central India. Resource Geology Special Issue, 15, 282–297.

Ramachandra, H.M., &Roy, A. (2001). Evolution of the Bhandara–Balaghat granulite belt along the southern margin of the Sausar mobile belt of central India. Proceedings of the Indian Academy of Sciences (Earth and Planetary Science) 110, 351–368.

Ramnathan, A., Bagchi, J., Panchapakesan, V.P., &Sahu, B.K. (1990). Sulphide mineralization at Malanjkhand—a study. Geological Survey of India Special Publications, 28, 585–598.

Regenauer-Lieb, K., Weinberg, R.F., &Rosenbaum, G. (2006). The effect of energy feedbacks on continental strength. Nature, 442, 67-70.

Roy, A., Kagami, H., Yoshida, M., Roy, A., Bandyopadhyaya, B.K., Chattopadhyay, A., Khan, A.S., Huin, A.K., &Pal, T. (2006). Rb-Sr and Sm-Nd dating of different metamorphic events from the Sausar Mobile Belt, central India: implications for Proterozoic crustal evolution. Journal of Asian Earth Sciences, 26, 61-76.

Rutter, E.H., & Maddock, R.H. (1992). On the mechanical properties of synthetic kaolinite/quartz fault gauge. Terra Nova, 4, 489-500.

Sarkar, S.C., Kabiraj, S., Bhattacharya, S., &Pal, A.B. (1996). Nature, origin and evolution of the granitoid-hosted early Proterozoic copper–molybdenum mineralization at Malanjkhand, central India. Mineralium Deposita, 31, 419–431.

Sekine, K., &Hayashi, K. (2009). Residual stress measurements on a quartz vein: a constraint on paleostress magnitude. Journal of Geophysical Research,114, B1404, doi:10.1029/2007JB005295.

Sikka, D. (1989). Malanjkhand: Proterozoic porphyry copper deposit, MP, India. Journal of Geological Society of India, 34, 487–504.

Sikka, D., &Nehru, C.E. (1997). Review of Precambrian porphyry Cu±Mo±Au deposits with special reference to Malanjkhand porphyry copper deposit, Madhya Pradesh, India. Journal of Geological Society of India, 49, 239–288.

Sikka, D.B., &Nehru, C.E. (2002). Malanjkhand copper deposit, India: is it not a porphyry type? Journal of Geological Society of India, 59, 339–362.

Sikka, D.B., Petruk, W., Nehru, C.E., &Zhang, Z. (1991). Geochemistry of secondary copper minerals from Proterozoic porphyry copper deposit, Malanjkhand, India. Ore Geology Reviews, 6, 257-290.

Stain, H.J., Hannah, J.L., Zimmerman, A., Markey, R.J., Sarkar, S.C., &Pal, A.B. (2004). A 2.5 Ga porphyry Cu-Mo-Au deposit at Malanjkhand, central India: implications for Late Archean continental assembly. Precambrian Research,134, 189-226.

Stein, H., Hannah, J., Zimmerman, A., &Markey, R. (2006). Mineralization and deformation of the Malanjkhand terrane (2,490-2,440 Ma) along the southern margin of the Central Indian Tectonic Zone. Mineralium Deposita, 40, 755-765.

Stipp, M., Stunitz, H., Heilbronner, R., &Schmid, S.M. (2002). Dynamic recrystallization of quartz: correlation between natural and experimental conditions. Geological Society of London Special Publication,200, 171-190.

Vishwakarma, R.K., (2001). Discussion on Cu–Mo–Au metallogeny associated with Proterozoic tectono-magmatism in Malanjkhand porphyry copper district, Madhya Pradesh. Journal of Geological Society of India, 57, 544–546.

West, G. (1991). A note on undulatory extinction of quartz in granite. Quarterly Journal of Engineering Geology and Hydrology, 24, 159-165.

***